IEEE Access
Multidisciplinary | Rapid Review | Open Access Journal

Received January 3, 2019, accepted February 4, 2019, date of publication March 15, 2019, date of current version March 29, 2019.

Digital Object Identifier 10.1109/ACCESS.2019.2900697

Optimization Design of a High-Coupling Split Reactor in a Parallel-Type Circuit Breaker

FATING YUAN[1], BO TANG[1], CAN DING[1], SHIHONG QIN[2], LI HUANG[1], AND ZHAO YUAN[3]

[1]Hubei Provincial Key Laboratory for Operation and Control of Cascaded Hydropower Station, College of Electrical Engineering and New Energy, China Three Gorges University, Yichang 443002, China
[2]School of Electrical Engineering and Information, Wuhan Institute of Technology, Wuhan 430205, China
[3]State Key Laboratory of Advanced Electromagnetic Engineering and Technology, Huazhong University of Science and Technology, Wuhan 430074, China

Corresponding author: Li Huang (huangli@ctgu.edu.cn)

This work was supported in part by the Hubei Provincial Key Laboratory for Operation and Control of Cascaded Hydropower Station, Three Gorges University, China, under Grant 2018KJX09.

ABSTRACT In this paper, in accordance with the breaker requirements of a parallel-type circuit breaker based on a high-coupling split reactor, the structure of a coupling reactor is proposed, and the influences of the inner radius, encapsulation height, air ducts width, and encapsulation number of the reactor on coupling factor is analyzed. The reactor design is optimized to minimize metal conductor usage, and the initial design parameters of the coupling reactor are selected based on equal height and heat flux of the coaxial encapsulations. Meanwhile, combined thermal and electromagnetic optimization method and heat load optimization are adopted considering a single-arm limiting current and two-arm flow current working conditions. The optimization results show that the metal conductor usage of the coupling reactor is only 63% compared to a design based on the initial design parameters, and the correctness of the optimization is verified by simulation results.

INDEX TERMS Parallel-type circuit breaker, coupling reactor, metal conductor usage, combined thermal and electromagnetic optimization, heat load optimization.

I. INTRODUCTION

With the rapid development of power system, fault current levels continuously increase, and when a circuit breaker cannot interrupt a fault current, it will directly affect the safe and stable operation of the system [1]–[3]. To reduce the influence of fault currents on power system, a parallel-type circuit breaker based on a high-coupling split reactor was proposed in [4] and [5], which increased the breaking capacity. The coupling reactor is an important piece of equipment, and its main performance parameters, such as the single-arm inductance, coupling factor and carrying current capacity, can be enhanced by increasing the encapsulation number, air ducts width and overall size of the structure, but these modifications lead to increased metal conductor usage. Therefore, to improve metal conductor utilization, a method to optimize the design of coupling reactors is needed.

Currently, the optimization of the design of a reactor mainly includes the following. (1) Electromagnetic optimization can be employed, as in [6], the minimum metal conductor usage can be obtained when the shape proportion of the reactor is given by $\alpha = 0.345$ and $\beta = 0.335$, where, α is the ratio of the height to the average diameter, and β is the ratio of the total thickness to the average diameter), in [7], A magnetic powder layer was added outside the metal conductor layer to increase the permeability, however, the thermal condition was not considered in [6] and [7], and the partial encapsulation temperature increase may over the operating limit. (2) Thermal optimization can also be used, as in [8]–[10], where methods that involve a uniform temperature increase, a uniform resistance and voltage, and a uniform resistance voltage drop are used in the design of a reactor, but the distribution of the temperature increase of each encapsulation is different, and the conductor cannot be fully utilized. In [11] and [12], combined thermal and electromagnetic optimization was adopted, and the distributions of the temperature increase of the inner encapsulation were basically the same, which can obviously reduce the metal conductor usage. However, a high-coupling spilt reactor has a single-arm limiting current and two-arm flow current, and the

The associate editor coordinating the review of this manuscript and approving it for publication was Mehdi Bagheri.

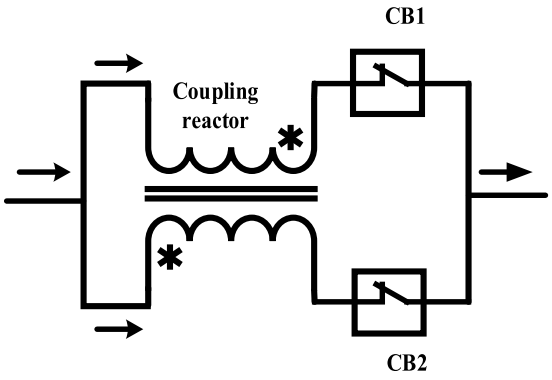

FIGURE 1. The topology structure of the parallel-type circuit breaker.

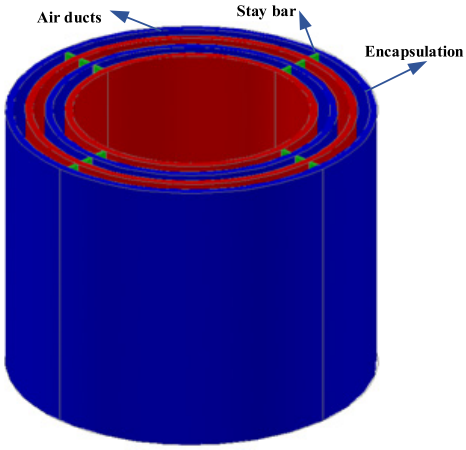

FIGURE 2. The basic structure of coupling reactor.

current distributions are different under the two working conditions. The optimization method mentioned above mainly focuses on the design of a traditional reactor, in which the encapsulation current directions are the same, so the method cannot be used in the design of a coupling reactor directly. In [13], a design method for a coupling reactor was proposed, but the electromagnetic and thermal characteristic were not involved, limiting its practical application.

In this paper, the structure of a coupling reactor is proposed based on the requirements of a parallel type circuit breaker, and the influences of the inner radius, encapsulation height, air ducts width and encapsulation number on the coupling factor are analyzed. According to an actual 220kV AC system, the initial design parameters of the coupling reactor are selected based on equal height and heat flux of the coaxial encapsulations, and an optimization method is proposed considering both electromagnetic and thermal aspects, which can obviously reduce metal conductor usage.

II. WORKING PRINCIPLE AND STRUCTURAL OF THE COUPLING REACTOR

A. WORKING PRINCIPLE

The topological structure of a parallel-type circuit breaker is shown in Fig.1, it mainly includes a coupling reactor and circuit breaker CB1 and CB2. Under normal conditions, a rated current passes through the two arms of coupling reactor, and the leakage inductance is small and has little effect on the power system. When the device needs to interrupt the fault current, the device is in one of situations: one situation involves the two-arm flow current, and the circuit breakers interrupt the fault current simultaneously; the other situation involves a single-arm limiting current, when one of the circuit breakers interrupts first, and the coupling reactor presents a large inductance, which can limit the fault current to the breaking capacity of a single circuit breaker, and finally break off the fault current.

B. STRUCTURAL TYPE OF COUPLING REACTOR

To meet the performance requirements for insulation, heat dissipation and high coupling for two working conditions, a dry-type air core reactor is selected for the coupling reactor because of its simple structure, light weight and good linearity, and its structure is shown in Fig.2.

The coupling reactor mainly includes multiple coaxial encapsulations, in which the odd encapsulations (1, 3, 5…) make up arm I, even encapsulations (2, 4, 6…) constitute arm II, adjacent encapsulations are wound in opposite directions, and each encapsulation is separated by air ducts and stay bar for insulation and heat dissipation.

C. THE INFLUENCE OF THE STRUCTURE PARAMETERS ON COUPLING FACTOR

The single-arm inductance needs to meet the requirement for the coupling reactor, which can be determined from the encapsulation voltage equation [14], as shown in equation (1).

$$\begin{cases} \sum_{j=1}^{m-1} W_i W_j f_{ij} I_j = L_1 I_{1tol}, \quad i,j = 1,3,5,m-1 \\ \sum_{j=2}^{m} W_i W_j f_{ij} I_j = L_2 I_{21tol}, \quad i,j = 2,4,6,m \end{cases} \tag{1}$$

where, W_i, I_i are the turn number and current of encapsulation i, L_1, L_2 are the I and II arm inductance, I_{1tol}, I_{2tol} are the I and II arm current, m is the encapsulation number, and f_{ij} is mutual inductance geometric coefficient.

According to inductance parameters of the coupling reactor, the coupling factor can be calculated.

$$k = \frac{M}{\sqrt{L_1 L_2}} \tag{2}$$

where, k is the coupling factor and M is the mutual inductance between two arms.

Fig.2 shows that the main influence factors on the coupling factor are the inner radius, encapsulation height, air ducts width and encapsulation number. Thus, the actual parameters of the coupling reactor are selected considering the influence of these factors, the encapsulation height is 1 m, the inner radius is 0.3 m, the air ducts width is 0.03 m, and the encapsulation number is 4. Meanwhile,

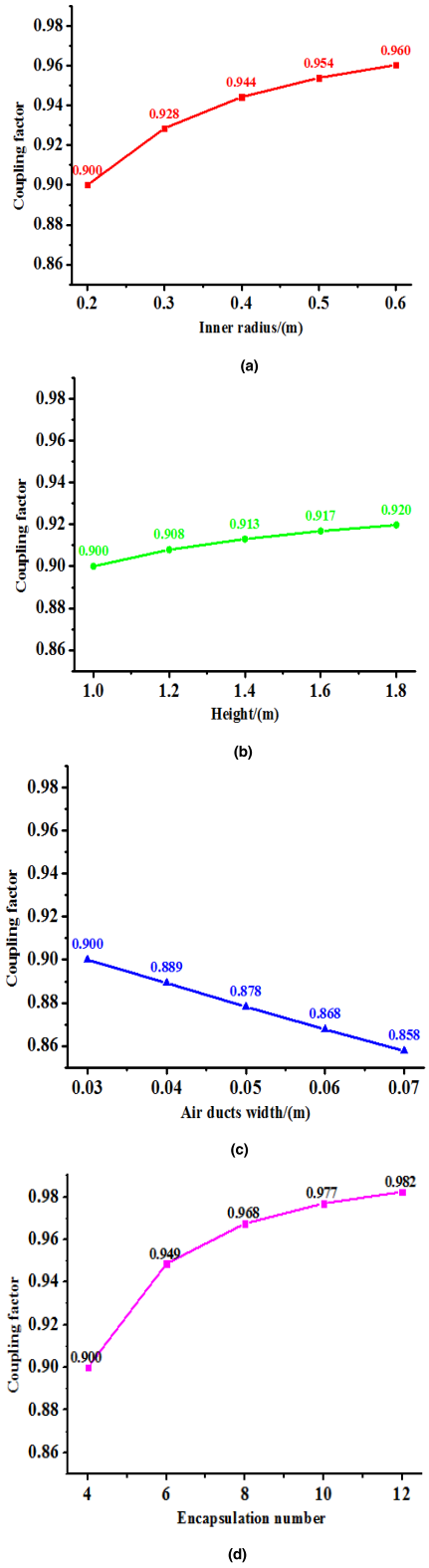

FIGURE 3. The change in the curve of the coupling factor for the different parameters. (a) The inner radius. (b) The encapsulation height. (c) The air ducts width. (d) The encapsulation number.

the design results of the inductances of arms I and II are the same, with a value of 3.1 mH, and the coupling factor is 0.9.

Assuming that the other parameters remain constant, the inner radius, encapsulation height, air ducts width and encapsulation number are selected as the independent variables (parameters), and the change in the curve of the coupling factor for the different parameters can be plotted, as shown in Fig.3.

Fig.3 shows that the coupling factor gradually increases with increasing inner radius, encapsulation height and encapsulation number, and the air ducts width has the opposite effect. At the same time, the encapsulation number has the greatest effect among the above parameters, and the coupling factor can reach 0.98 when the encapsulation number is 10.

III. OPTIMIZATION OF THE DESIGN OF THE COUPLING REACTOR

The optimization goal for the coupling reactor is to minimize the metal conductor usage. The preconditions are that the single-arm inductance, coupling factor and temperature increase must meet the performance requirements of the coupling reactor, so the object function can be expressed as [15]:

$$min\ Mass = \pi\rho_0 \sum_{i=1}^{m} W_i D_i S_i \tag{3}$$

where, $Mass$ is the total mass of metal conductor, ρ_0 is the mass density, W_i, D_i, S_i are the turn number, diameter, and cross sections of encapsulation i.

A. THE INITIAL DESIGN PARAMETERS OF THE COUPLING REACTOR

According to the actual parameters of a 220 kV AC system and the requirements of a parallel-type circuit breaker, the main parameters of the coupling reactor are shown in Tab.1.

From Tab.1, it can be seen that the inductances of arms I and II are the same, and the coupling factor is approximately 1; thus, the coupling reactor can be made equivalent to an ordinary reactor, which is similar to the situation of single-arm limiting current. The equivalent model is shown in Fig.4.

The inductance matrix can be written as in equation (4).

$$M = \begin{bmatrix} M_{1,1}, & M_{1,2} & \cdots & M_{1,m} \\ M_{2,1}, & M_{2,2} & \cdots & M_{2,m} \\ \vdots & \ddots & & \vdots \\ \vdots & & M_{x,y} & \vdots \\ \vdots & & \ddots & \vdots \\ M_{m,1}, & M_{m,2} & \cdots & M_{m,m} \end{bmatrix} \quad (x, y = 1, 2 \cdots m) \tag{4}$$

Equal height and heat flux of the coaxial encapsulations are selected in designing the reactor. When adopting this method, the encapsulation height, air ducts width and heat flux of the encapsulation are basically the same, providing precondition conditions for the optimization of the design of the coupling reactor.

TABLE 1. The main parameters of coupling reactor.

Parameters	VALUE
Rated voltage (kV)	220
Rated current (A)	3150
I arm inductance (mH)	3.1
II arm inductance (mH)	3.1
Coupling factor	⩾0.98
Temperature rise (℃)	⩽90

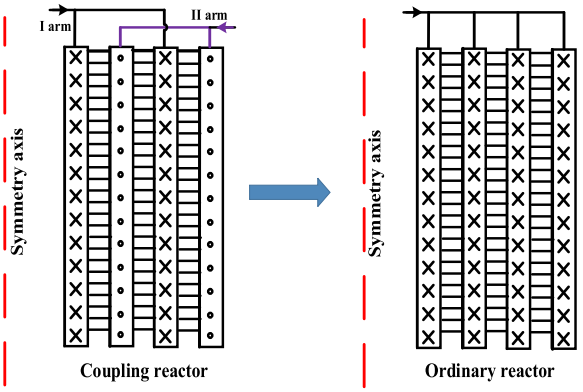

FIGURE 4. The equivalent model of the coupling reactor.

According to parameters requirements and design method for the coupling reactor, the initial parameters are achieved. The inner radius is 0.5 m, the height is 1.2 m, the air ducts width is 0.025 m, the encapsulation number is 10, and the coupling factor is 0.98. Meanwhile, the metal conductor usage is 6.3 t (the material is aluminum), and the temperature increase is approximately 45 °C.

B. COMBINED THERMAL AND ELECTROMAGNETIC OPTIMIZATION

The realization of combined thermal and electromagnetic optimization should be in accordance with the conservation of inductance and maximum temperature increase.

(1)Temperature increase conservation: the heat and heat dissipation conditions of the inner encapsulation are basically the same based on equal height and heat flux, so the encapsulation-air duct unit is selected to reflect the temperature increase distribution of the reactor. Combined with the knowledge of heat transfer in the vertical pipe, the maximum temperature increase can be written as [12]:

$$\Delta T_{max} = \frac{2q_w H}{d\bar{u}\rho C_p} + \frac{2q_w d}{\lambda Nu} \tag{5}$$

where, $\Delta Tmax$ is the maximum temperature rise, q_w is the heat flux conducted from the encapsulation surface to air ducts, H is the encapsulation height, d is the air ducts width, u is the average velocity of fluid, ρ is the fluid density, C_p is the specific heat at constant pressure, Nu is the Nusselt number of fluid in air ducts, and λ is the heat conductivity coefficient.

(2) Inductance conservation: from the point of view of inductance, an air core reactor with multiple coaxial encapsulations is essentially the same as thick wall coils; thus, a single thick wall coil is selected to reflect the inductance of the reactor, which can be written as [6]:

$$L_0 = \frac{7.85 W_{av}^2 D_{av}^2}{3D_{av} + 9Thi + 10H} \times 10^{-6} \tag{6}$$

where, W_{av}, D_{av}, H and THi are the average turn number, average diameter, height and total thickness of thick wall coils respectively.

Supposing the initial design parameter is x_0, the values become x after adjustment, the definition about k_x can be written as $k_x = x/x_0$.

To realize combined thermal and electromagnetic optimization considering the changes of encapsulation number and air ducts width, the structure function is essential, as shown in equation (7).

$$\begin{cases} THi = m(a+d) \\ H = W_{av} \cdot b \end{cases} \tag{7}$$

With the equal height and heat flux of the coaxial encapsulations, combined with equations (5) and (7), the total constraint conditions of the combined thermal and electromagnetic optimization method can be written as [16]:

$$\begin{cases} I_i^2 \dfrac{W_i}{S_i H_i} = I_j^2 \dfrac{W_j}{S_j H_j} \\ H_i = H_j = H \quad (i, j = 1, 2, \cdots, m) \\ k_a = \dfrac{1}{k_b^2} \dfrac{\lambda Nu k_{Nu} H k_b k_{W_{av}} + d^2 \bar{u} k_{\bar{u}} \rho C_p}{\lambda NuH + d^2 \bar{u} \rho C_p} \dfrac{1}{k_{Nu} k_{\bar{u}}} \\ k_{W_{av}} = \dfrac{W_{av}^{'}}{W_{av}} = \sqrt{\dfrac{(3 + 9\alpha' + 10\beta')}{(3 + 9\alpha + 10\beta)} k_{D_{av}}^{-1}} \\ THi = m(a+d) \\ H = W_{av} \cdot b \end{cases} \tag{8}$$

where, α and β are the initial geometry factors, α' and β' are the optimized geometry factors, a and b are the radial width and single turn axial height, k_{ad} is the ratio value of a and d.

Combined with the initial design parameters of coupling reactor and the physical characteristic of fluid in the air ducts, the proportionality factor of metal conductor usage can be rewritten based on equation (3), where, the value of α is 1.5, and β is 0.2 [16].

$$k_{Mass} = f(k_d, k_m) \tag{9}$$

In equation (9), it can be seen that the proportionality factor of metal conductor usage, k_{Mass}, is determined by two independent variables, k_d and k_m, thus, the optimization curve can be plotted, as shown in Fig.5. Where, the range of k_d is from 0.9 to 1.1, and the k_m ranges from 0.8 to 1.2.

In Fig.5, the k_{Mass} can be minimized when $k_d = 1.1$ and $k_m = 1.2$, the optimal encapsulation number, air ducts width and structure size can be achieved from the optimization curve, and the main parameters are as follows: the inner radius is 0.3 m, the height is 1.84 m, the air ducts width is 0.0275 m, and the encapsulation number is 12. Meanwhile, the metal conductor usage is 4.1 t.

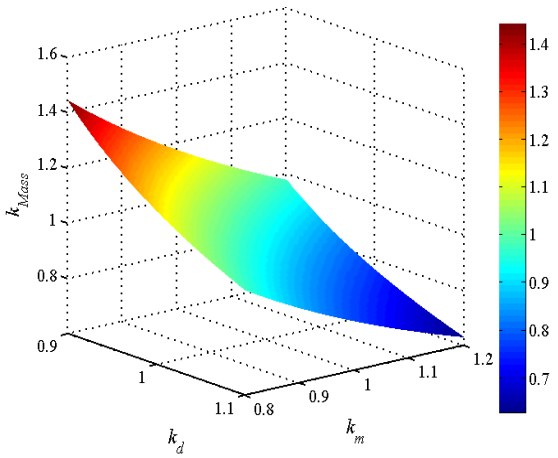

FIGURE 5. The combined thermal and electromagnetic optimization curve.

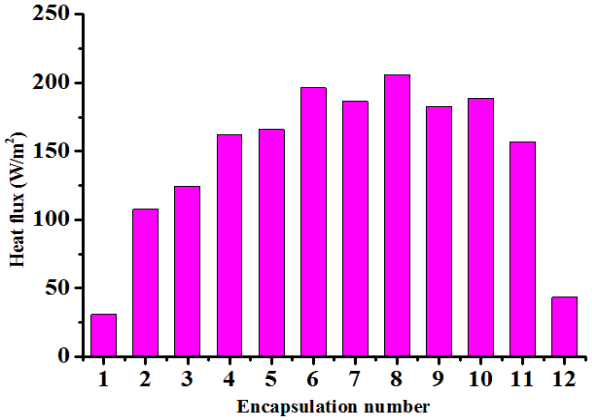

FIGURE 6. The heat flux distribution of encapsulation surface.

C. THE HEAT LOAD OPTIMIZATION

The combined thermal and electromagnetic optimization method merely considers the situation of a single-arm limiting current. In an actual operation process of a coupling reactor, a rated current passes through two arms of a coupling reactor. The current directions are different between adjacent encapsulations, and the inductance matrix can be written as:

$$M = \begin{bmatrix} M_{1,1}, & -M_{1,2} & \cdots & -M_{1,m} \\ -M_{2,1}, & M_{2,2} & \cdots & M_{2,m} \\ \vdots & \ddots & & \vdots \\ \vdots & & (-1)^{|x-y|} M_{x,y} & \vdots \\ \vdots & & \ddots & \vdots \\ -M_{m,1}, & M_{m,2} & \cdots & M_{m,m} \end{bmatrix} \quad (x, y = 1, 2, 3, \cdots m) \quad (10)$$

According to the combined thermal and electromagnetic optimization results, the heat flux distribution of the encapsulation surface can be calculated, as shown in Fig.6.

In Fig.6, the heat flux of the inner encapsulation surface are basically the same, but the outer encapsulation (including encapsulation 1, 2 and encapsulation 12) are obviously lower in terms of heat flux than the inner encapsulations, so the metal conductor is not fully utilized for the outer encapsulations.

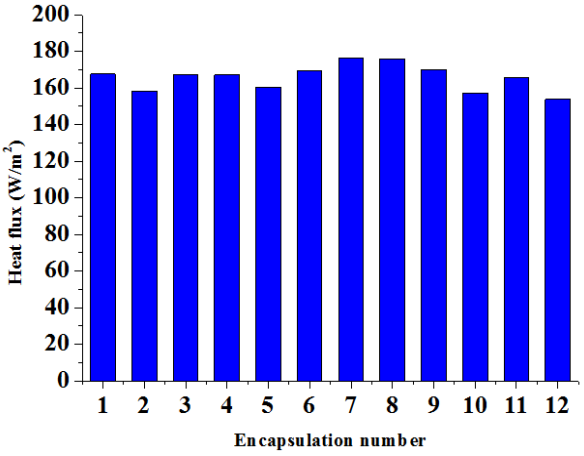

FIGURE 7. The heat flux distribution of encapsulation surface with the heat load optimization method.

Taking the outer encapsulations of the coupling reactor as the object to be optimized, when the heat flux of an outer encapsulation is equal to that of an inner encapsulation under a two-arm flow current, the heat dissipation conditions of each encapsulation are basically the same, so the equation constraint condition can be written as:

$$qw_c = qw \quad (c = 1, 2, 12) \quad (11)$$

where, qw is the heat flux of the inner encapsulation, and qw_c is the heat flux of the outer encapsulation.

According the heat load optimization results, the equal height and unequal heat flux are adopted considering the heat flux of each encapsulation is different, and the constraint conditions are:

$$\begin{cases} \sum_{j=1}^{m} W_i W_j f_{ij} I_j = L_0 I_0 & i = 1, 2, \cdots m \\ k_{c,i} I_i^2 W_i / S_i = k_{c,j} I_j^2 W_j / S_j & \\ H_i = H_j = H & i, j = 1, 2, \cdots m \end{cases} \quad (12)$$

where, $k_{c,\,i}$ is the adjustment factor of heat flux for encapsulation i.

From the equation (12), the optimization design results of the coupling reactor can be obtained, the metal conductor usage is 4.0 t, and it is only 63% compared with the initial design parameters. The heat flux distribution of the encapsulation surface can also be calculated, as shown in Fig.7.

In Fig.7, it can be found that the heat flux of each encapsulation are basically the same, so the carrying capacity of outer encapsulation are obviously increased with the heat load optimization method.

The optimization design of the coupling reactor includes two main aspects: combined thermal and electromagnetic optimization and heat load optimization. The overall optimization flowchart is shown in Fig.8.

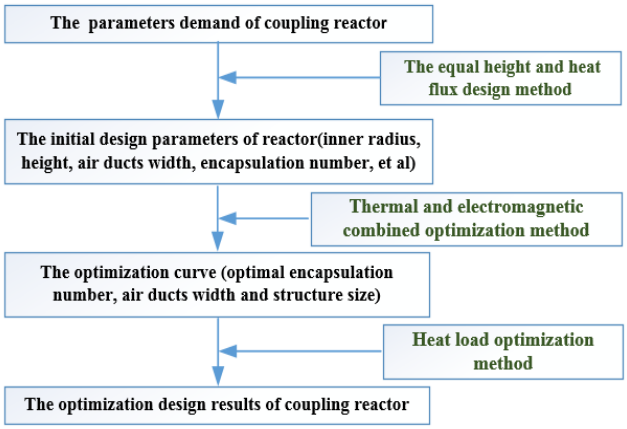

FIGURE 8. The overall optimization flowchart.

IV. SIMULATION VERIFICATION

To verify the correctness of design results for the single-arm inductance, coupling factor and temperature increase, the electromagnetic field and temperature field simulation models are established.

A. INDUCTANCE AND COUPLING FACTOR

According to the design results of the coupling reactor, a field-circuit coupled finite element method is adopted to calculate the single-arm inductance and coupling factor [17]–[19], the circuit model and coil model are shown in Fig.9.

Some simplification has been done, the coupling reactor is equivalent to axisymmetric model, the encapsulation height, air ducts width, turn number and radial width are setting accordance with the actual structure size, the metal conductor material and insulation material are based on those of actual materials.

The boundary conditions are essential to the simulation calculation, and the setting are as follows: the left boundary line of the model is set as the symmetry axis, and the upper, lower and right boundary lines are set as balloon boundary.

The voltage waveform of the single-arm limiting current can be obtained when the current source is set at 160.65 kA, as shown in Fig.10.

Similarly, the voltage waveform with two-arm flow current can be obtained when the current source is set at 216.75 kA, as shown in Fig.11.

It can be calculated that the inductances of arms I and II are 3.1 mH and 3.1 mH, respectively, and the coupling factor is 0.98; so the simulation results show that the single-arm inductance and coupling factor meet the performance requirements of the coupling reactor.

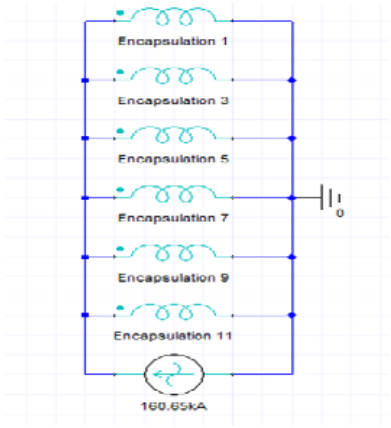

(a)

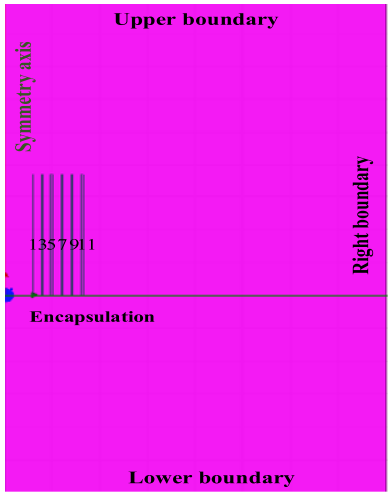

(b)

FIGURE 9. The field-circuit coupled simulation model. (a) The circuit model. (b) The coils model.

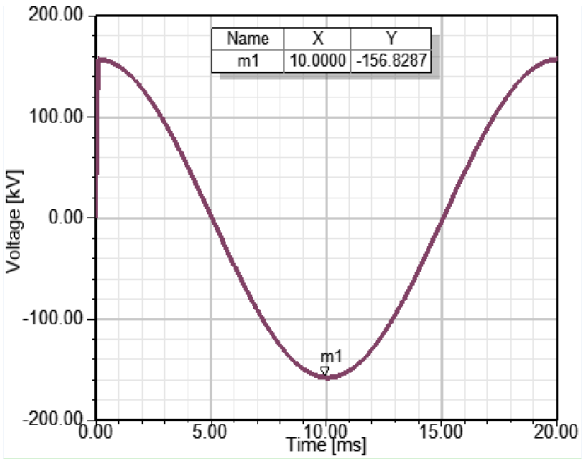

FIGURE 10. The voltage waveform of I arm limiting current.

B. TEMPERATURE INCREASE

Temperature increase is an important parameter of the coupling reactor. The FEM (finite element method) is widely used to calculate the temperature rise, and the correctness of the approach described in this paper has been verified by experimental results [20], [21]. According to the optimization design results of the coupling reactor, a fluid-thermal coupled

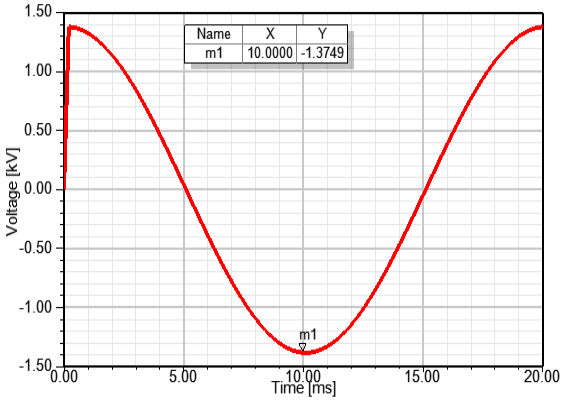

FIGURE 11. The voltage waveform with two-arm flow current.

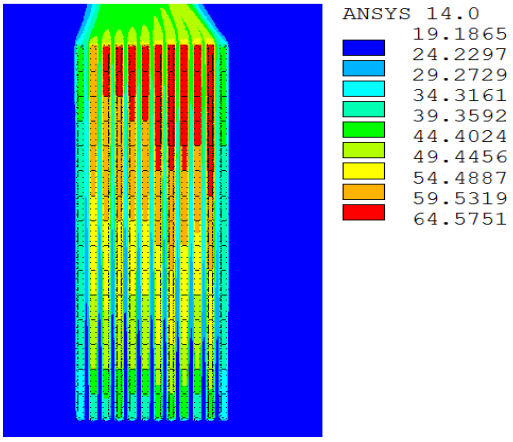

FIGURE 12. The temperature field simulation result.

finite element model is established based on the ANSYS simulation platform, and some simplification has been performed.

Considering only a steady-state thermal process, the influences of the spider arm and stay bar on the temperature increase of the reactor are ignored. The reactor is equivalent to a 2D axisymmetric model, and the air ducts width, encapsulation height and radial width are basically identical to the design parameters. Meanwhile, the size and properties of the insulation materials are set to be proportional to the parameters of the actual materials; the whole computational domain is the 3 times the radial length and 2.5 times the axial height of the reactor in the model. The governing equation, heat source loading, mesh generation and boundary condition settings are taken from the literature [22].

The temperature field simulation result is achieved when a two-arm flow current is used, as shown in Fig.12.

In Fig.12, it can be seen that the temperature increase of each encapsulation are basically the same, the maximum temperature increase is 44.6 °C, which is basically equal to the temperature increase associated with the initial design parameters, so the design results meet the flow capacity requirements of the coupling reactor.

V. CONCLUSION

The structure of a coupling reactor is given according to the requirements of a parallel-type circuit breaker, and an optimization method is proposed to minimize metal conductor usage. The following conclusions can be obtained.

(1) The coupling factor gradually increases with increasing inner radius, encapsulation height and encapsulation number, and the coupling factor reaches 0.98 when the encapsulation number is 10, but the air ducts width has the opposite effect.

(2) The combined thermal and electromagnetic optimization, heat load optimization are used in the design of the coupling reactor. The metal conductor usage is only 63% compared with a design based on the initial design parameters, which can significantly improve the utilization of metal conductors.

REFERENCES

[1] J. Lee and S.-K. Joo, "Economic assessment method for superconducting fault current limiter (SFCL) in fault current-constrained power system operation," *IEEE Trans. Appl. Supercond.*, vol. 23, no. 3, Jun. 2013, Art. no. 5601104.

[2] G.-H. Moon, Y.-M. Wi, K. Lee, and S.-K. Joo, "Fault current constrained decentralized optimal power flow incorporating superconducting fault current limiter (SFCL)," *IEEE Trans. Appl. Supercond.*, vol. 21, no. 3, pp. 2157–2160, Jun. 2011.

[3] Y. Chai, C. Jiang, K. Zhang, and S. Xu, "Safe operation improvement of an electrical power system by superconducting fault current limiters," in *Proc. Chin. Control Decis. Conf. (CCDC)*, Yinchuan, China, May 2016, pp. 1310–1314.

[4] Z. Guo *et al.*, "Interrupting characteristics of paralleled SF_6 circuit breakers with a highly coupled split reactor," *IEEE Trans. Compon., Packag., Manuf. Technol*, vol. 7, no. 5, pp. 768–776, May 2017.

[5] D.-Y. Qu, R. Chen, J.-Wu, F.-T. Wan, J.-X. Liu, and Y. Wang, "Development of high coupled split reactor for large capacity parallel circuit breaker device," *Transformer*, vol. 54, no. 7, pp. 25–32, May 2017.

[6] J.-X. Huang, Z.-H. Xiao, and G.-K. Chen, "The calculation and design of air reactor," *Electric Drive*, no. 5, pp. 46–55, Oct. 1991.

[7] L.-F. Luo, S.-Q. Zhao, J.-Z. Xu, L.-L. Wei, Y.-G. Lou, and H.-B. Chen, "Design of large inductance power cable," *High Voltage Eng.*, vol. 41, no. 8, pp. 2635–2642, Aug. 2015.

[8] Y. Li, Z. Zhang, L. Li, G. Li, and M. Jiang, "Calculation and design of dry-type air-core reactor," *Energy Power Eng.*, vol. 5, no. 4, pp. 1101–1104, Jul. 2013.

[9] F. Chen, Y.-Z. Zhao, and X.-K. Ma, "Optimum design of dry-type air-core reactor based on design variable reconstruction," *Proc. CSEE*, vol. 29, no. 21, pp. 99–106, Jul. 2009.

[10] Y. Zhao, B. Kang, and X. Ma, "Optimization model of dry type air-core reactor based on balance of additional constraints," *Trans. China Electrotech. Soc.*, vol. 25, no. 11, pp. 80–84, Nov. 2010.

[11] Z. Yuan, J.-J. He, Y. Pan, X.-G. Yin, C.-J. Luo, and S.-Z. Chen, "Research on electromagnetic efficiency optimization in the design of air-core coils," *Int. Trans. Elect. Energy Syst.*, vol. 25, no. 5, pp. 789–798, Jan. 2014.

[12] F. Yuan, Z. Yuan, Y. Wang, J. Liu, H. Su, and J. He, "Research of electromagnetic and thermal optimization design on air core reactor," *IEEJ Trans. Elect. Electron. Eng.*, vol. 13, no. 5, pp. 725–731, May 2018.

[13] Z. Yuan, "Research of thermal and electromagnetic optimization design on air-core power reactors with paralleled cylindrical coils," Ph.D. dissertation, School Elect. Electron. Eng., Huazhong Univ. Sci. Technol., Wuhan, China, 2014.

[14] Y. Li, Z.-H. Zhang, L.-X. Zhu, and M.-H. Jiang, "Calculation and design of dry-type air-core reactor," *Transformer*, vol. 50, no. 10, pp. 1–6, Oct. 2013.

[15] C. Zhang, Y. Zhao, J. Zou, and X. Ma, "A diversity-guided modified QPSO algorithm and its application in the optimization design of dry-type air-core reactors," *Proc. CSEE*, vol. 32, no. 18, pp. 108–117, Jun. 2012.

[16] F. Yuan *et al.*, "Thermal and electromagnetic combined optimization design of dry type air core reactor," *Energies*, vol. 10, no. 12, p. 1989, Dec. 2017.

[17] W. Ziqiang, Y. Zhongdong, W. Lan, K. Ning, W. Miaomiao, and W. Zhijian, "Study on field-circuit coupling model of saturated reactor based on finite elements theory," in *Proc. Int. Conf. Energy Environment Technol.*, Guilin, China, 2009, pp. 313–316.
[18] Z. Wang, Z. Yin, Y. Po, and L. Key, "The finite elements analysis on magnetic field of controllable saturated reactor," in *Proc. Int. Conf. Power Electron. Drive Syst. (PEDS)*, Taipei, Taiwan, Nov. 2009, pp. 364–368.
[19] X. Yan and C. Yu, "Magnetic field analysis and circulating current computation of air core power reactor," in *Proc. Asia-Pacific Power Energy Eng. Conf.*, Wuhan, China, Mar. 2011, pp. 1–3.
[20] Z.-P. Jiang, X.-S. Wen, Y. Wang, R.-Z. Chen, J.-F. Cao, and T.-T. Chen, "Test and coupling calculation of temperature field for UHV dry-type air-core smoothing reactor," *Proc. CSEE*, vol. 35, no. 20, pp. 5344–5350, Oct. 2015.
[21] F. Chen, Y. Zhao, and X. Ma, "An efficient calculation for the temperature of dry air-core reactor based on coupled multi-physics model," in *Proc. 6th Int. Conf. Electromagn. Field Problems Appl.*, Dalian, China, Jun. 2012, pp. 1–4.
[22] F. T. Yuan, Z. Yuan, J. X. Liu, Y. Wang, W. X. Mo, and J. J. He, "Research on temperature field simulation of dry type air core reactor," in *Proc. 20th Int. Conf. Elect. Mach. Syst. (ICEMS)*, Sydney, NSW, Australia, Aug. 2017, pp. 1–5.

FATING YUAN was born in Hubei, China. He received the B.S. and M.S. degrees from the Wuhan Institute of Technology, in 2011 and 2014, respectively, and the Ph.D. degree from the Huazhong University of Science and Technology. He is currently with China Three Gorges University. His research interest includes high-voltage reactors.

BO TANG was born in Hubei, China. He received the M.S. degree from China Three Gorges University and the Ph.D. degree from the Huazhong University of Science and Technology, in 2011. He is currently with China Three Gorges University, as a Professor. His research interests include power transmission line engineering and electromagnetic environment of power systems.

CAN DING was born in Shandong, China. He received the B.S. and M.S. degrees from Xi'an Jiaotong University, in 2005 and 2010, respectively, and the Ph.D. degree from the Huazhong University of Science and Technology. He is currently with China Three Gorges University. His research interests include high-voltage electric appliance and equipment.

SHIHONG QIN was born in Hubei, China. He received the Ph.D. degree from the Huazhong University of Science and Technology, in 1998. He is currently with the Wuhan Institute of Technology. His research interests include information processing, intelligent electrical apparatus, and pulse power technology.

LI HUANG was born in Hubei, China. He received the M.S. degree from China Three Gorges University, in 2006, and the Ph.D. degree from Uiduk University, in 2016. He is currently with China Three Gorges University. His research interests include high-voltage technology, applied superconductivity, and electromagnetic analysis.

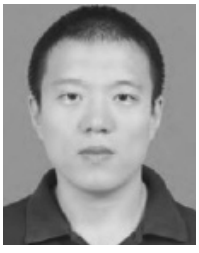

ZHAO YUAN was born in Henan, China. He received the Ph.D. degree from the Huazhong University of Science and Technology, in 2014. He is currently with the Huazhong University of Science and Technology. His research fields include high-voltage switching equipment and high-voltage reactors.